Title	Metal-binding domains and the metal selectivity of the vanadium(IV)-binding protein VBP-129 in blood plasma
Author(s)	Ueki, Tatsuya; Nakagawa, Takafumi; Michibata, Hitoshi
Citation	Journal of Inorganic Biochemistry , 116 : 70 - 76
Issue Date	2012-11
DOI	10.1016/j.jinorgbio.2012.08.003
Self DOI	
URL	https://ir.lib.hiroshima-u.ac.jp/00039964
Right	Copyright (c) 2012 Elsevier Inc. All rights reserved. This manuscript version is made available under the CC-BY-NC-ND 4.0 license http://creativecommons.org/licenses/by-nc-nd/4.0/
Relation	

Metal-binding domains and the metal selectivity of the vanadium(IV)-binding protein VBP-129 in blood plasma

Tatsuya Ueki [*], Takafumi Nakagawa, and Hitoshi Michibata

Molecular Physiology Laboratory, Department of Biological Science, Graduate School of Science, Hiroshima University, 1-3-1 Kagamiyama, Higashi-Hiroshima 739-8526, Japan.

[*] Corresponding author: Tel.&Fax.: +81 82 424 7437; *E-mail address*: ueki@hiroshima-u.ac.jp (T. Ueki).

Abstract

Ascidians are well known to accumulate extremely high levels of vanadium in their blood cells. Several key proteins related to vanadium accumulation and physiological function have been isolated from vanadium-rich ascidians. Of these, vanadium(IV)-binding protein-129 (VBP-129) is a unique protein that has been identified from the blood plasma of an ascidian *Ascidia sydneiensis samea*, but its metal binding domains are not known. In this study, several deletion and point mutants of VBP-129 were generated, and their metal binding abilities were assessed by immobilized metal ion affinity chromatography (IMAC) and electron spin resonance spectroscopy (ESR). The internal partial protein, VBP-Int41, did not bind to V^{IV}, but the two constructs, VBP-N52 and VBP-Int55, added with additional 11 or 14 neighboring amino acids bound to V^{IV}. Mutations for cysteine-47 and lysine-50 in VBP-Int55 diminished V^{IV}-binding in VBP-Int55, suggesting that these amino acid residues play important roles in binding V^{IV}. ESR titration analysis revealed that VBP-129, VBP-N52 and VBP-Int55 could bind to 6, 3 and 2 V^{IV} ions, respectively. ESR spectrum analysis indicated a N_2O_2 coordination geometry, which is similar to Vanabins. The cysteines may contribute to the maintenance of the three-dimensional structure that is necessary for binding V^{IV} ions. VBP-129 did not have a V^{V}-reductase activity, as expected from its tissue localization in blood plasma. This study provided the evidences that VBP-129 possesses V^{IV}-binding domains that make a similar coordination to V^{IV} as those by Vanabins but VBP-129 acts solely as V^{IV}-chaperon in blood plasma.

Key words

Vanadium; Ascidian; Metal-binding Protein; Site-directed mutagenesis

1. Introduction

The unusual ability of ascidians to accumulate high levels of vanadium ions has been attracting attention in biological and chemical disciplines for a century [1]. Vanadium ions are stored in the vacuoles of vanadium-containing cells called vanadocytes, where high levels of protons and sulfate ions are also found. The maximum concentration of vanadium can reach 350 mM in vanadocytes of *Ascidia gemmata*, belonging to the class Ascidiidae, and is thought to be the highest metal accumulation factor of any living organism (10^7 times against its concentration in natural sea water, 35 nM). Vanadium is usually found in the +5 oxidation state (HVO_4^{2-} or $H_2VO_4^-$; V^V) in the natural aquatic environment, but most of these ions are reduced to +3 (V^{3+}; V^{III}) via the +4 state (VO^{2+}; V^{IV}) during assimilation [2, 3]. Additionally, most vanadium ions are stored in the vacuoles of signet ring cells, a type of blood cell, and are often referred to as vanadocytes [4, 5].

Ongoing research over the last two decades has identified many proteins involved in the process of accumulating and reducing vanadium in vanadocytes, blood plasma, and the digestive tract of ascidians, such as vacuolar-type H^+-ATPase [6-8], the chloride channel [9], the sulfate transporter [10], enzymes of the pentose-phosphate pathway [11-14], the glutathione transferase [15], Vanabins [16-18], and a vanadium transporter [19].

Two types of vanadium-binding proteins that are expressed in blood plasma have been identified in *A. sydneiensis samea*. One protein was identified as a member of the Vanabin family, VanabinP, and its recombinant form binds a maximum of 13 V^{IV} ions per molecule with a K_d of 2.8×10^{-5} M [18]. The other protein was named VBP-129; it binds to V^{IV} ions as well as to Fe^{III}, Co^{II}, Cu^{II}, and Zn^{II} ions [20]. A truncated form of VBP-129 that does not bind to V^{IV} was also discovered, which has been called VBP-88 for its lack of 41 amino acid residues [20]. But, the properties such as binding number and coordination geometry in VBP-129 have not been revealed.

In this study, we sought to reveal the position and property of V^{IV}-binding domain(s) of VBP-129 as well as the contribution of crucial amino acids for the binding of V^{IV}. According to the differential sequence between full-length VBP-129 and its spontaneous truncated form VBP-88, several deletion and point mutants of VBP-129 were created using PCR amplification and *in vitro*

site-directed mutagenesis. Their metal binding abilities were assessed by IMAC and ESR. ESR measurements were conducted to reveal binding number and coordination geometry of V^{IV} to VBP-129. Since reductase activity was not detected, VBP-129 seemed to act solely as a V^{IV}-carrier protein in blood plasma.

2. Material and methods

2.1 Construction of expression plasmids

Deletion mutants of VBP-129 were constructed by PCR amplification using a VBP-129 expression plasmid [20] as the template. Primer sets and templates used are listed in Table 1. PCR reactions consisted of 100 ng plasmid DNA, 200 pmol of each primer, each dNTP at 0.2 mM, 1× reaction buffer, and 2.5 units of *Taq* DNA polymerase (TaKaRa, Inc.) in a total volume of 50 μL. Amplification was performed with an initial denaturation at 94°C for 2 min, 30 cycles of 94°C for 30 s, 55°C for 30 s, and 72°C for 30 s, and a final extension at 72°C for 5 min. After purification by agarose gel electrophoresis and cloning into pBluescript/*Eco*RV/dT vector, the nucleotide sequence was confirmed using an ABI 3130 automated DNA sequencer (Applied Biosystems Japan Ltd.) at the Natural Science Center for Basic Research and Development, Hiroshima University (N-BARD).

Each plasmid DNA was digested with restriction enzymes to excise the amplified fragments. These fragments were ligated into the multiple cloning sites of the expression vector pMAL-c2X (New England BioLabs), which contains the *lac* promoter and a coding region for MBP. Each plasmid was introduced into *Escherichia coli* BL21 for protein expression.

Plasmid vector and host *E. coli* strain for expressing another vanadium-binding protein, Vanabin1, were the same ones as used in our previous work [16].

2.2 In vitro site-directed mutagenesis

Site-directed mutagenesis of the coding region of VBP-129 and VBP-Int55 was conducted by a

PCR-based *in vitro* procedure based on the manufacturer's protocol as described previously [21], using the plasmid vectors pMal-p2X with the VBP-129 insert and pMal-c2X with the VBP-Int55 insert as templates. The combination of primer sets and template DNAs are listed in Table 1. Target residues were cysteine-47 (TGC) and lysine-50 (AAA) in the VBP-Int55 amino acid sequence, and cysteine-80 (TGC) and lysine-83 (AAA) in the VBP-129 amino acid sequence (Fig. 1). The cysteine and lysine were substituted by serine (AGC) and alanine (GCA), respectively. Each primer pair had a mutagenizing codon, which was flanked by complementary regions of 9-12 nucleotides.

The PCR reaction mix contained 50 ng of plasmid DNA, 35 pmol of each mutagenizing primer, 1× *Pfu* reaction buffer (Stratagene), 0.2 mM of each dNTP, and 2.5 units of *Pfu* turbo DNA polymerase (Stratagene) in a total volume of 50 µL. After incubation at 95°C for 30 s, 12 cycles of 30 s at 95°C, 60 s at 55°C, and 14 min at 68°C were conducted. After chilling on ice for 2 min, the restriction enzyme *Dpn*I (20 units) was added and the reaction was incubated at 37°C for 60 min. An aliquot (1 µL) was used to transform competent *E. coli* DH5α cells. Following selection on plates LB-Amp medium with ampicillin, nucleotide sequences were determined as mentioned above. Each plasmid was introduced into *E. coli* BL21 for protein expression.

2.3 Recombinant protein expression

Recombinant proteins were prepared as described previously [20]. Briefly, *E. coli* cells transformed with each plasmid DNA were incubated overnight at 37°C in 200-mL LB-Amp medium containing ampicillin (50 µg/mL). After dilution with 1,800-mL fresh LB-Amp medium, 0.1 mM IPTG was added and the culture was incubated at 37°C for 6 h. The fusion protein was purified by amylose resin column chromatography and digested with 1:500 (w/w) of factor Xa (Haematologic Technologies Inc.) at 4°C for 18 h. The excised protein was then purified by DEAE Sephacel anion exchange chromatography (GE Healthcare Bioscience Japan). Trace metal ions were removed by dialysis against approximately 100 volumes of Tris-EDTA solution (100 mM NaCl, 25 mM Tris-HCl, 50 mM EDTA, pH 7.5). EDTA was removed by dialysis three times against approximately 100 volumes of binding buffer for each assay. The protein concentration was measured with the BioRad

protein assay kit (Bio-Rad Laboratories, Inc.) using BSA as a standard.

2.4 Immobilized metal ion affinity chromatography (IMAC)

All buffers were prepared from DW and ultrapure-grade reagents, and degassed for 10 min under vacuum before use. Calcium chloride (Ca^{II}; $CaCl_2 \cdot 2\ H_2O$), cobalt sulfate (Co^{II}; $CoSO_4 \cdot 7\ H_2O$), copper chloride (Cu^{II}; $CuCl_2 \cdot 2\ H_2O$), iron chloride (Fe^{III}; $FeCl_3$), magnesium chloride (Mg^{II}; $MgCl_2 \cdot 6\ H_2O$), manganese chloride (Mn^{II}; $MnCl_2$), vanadyl sulfate (V^{IV}; $VOSO_4.n\ H_2O$, n = 3-4), and zinc chloride (Zn^{II}; $ZnCl_2$) were used as 99.9% pure reagents purchased from Wako Pure Chemicals, Japan. All these metal compounds were dissolved in DW at 0.1 M. Given that Fe^{III} and Zn^{II} solutions contain precipitates, only supernatants were used after settling the solutions for several minutes. Hence the concentration of Fe^{III} and Zn^{II} are slightly lower then the initial concentration of 0.1M, but they were enough to charge the chelating resin. Chelating Sepharose FF resin (GE Healthcare Bioscience Japan) was washed three times with water and mixed with each metal solution in a 2.0-mL plastic tube for 15 min (125 μL bed volume per each tube). The resin was washed three times with DW and twice with binding buffer (100 mM NaCl, 20 mM Na_3PO_4, pH 7.2). The protein in the binding buffer (~300 μg/mL, 500 μL) was mixed with the resin by rotation for 30 min at 4°C. Non-bound proteins were removed by centrifugation and the resin was washed three times with binding buffer. Bound proteins and metal ions were eluted with elution buffer (100 mM NaCl, 20 mM Na_3PO_4, 50 mM EDTA, pH 8.0, 400 μL). Non-bound and bound protein fractions were analyzed by SDS-PAGE and CBB staining.

2.5 ESR measurements

ESR measurements on Vanabin1 were done according to our previous study [22], while measurements on VBP-129 and its derivatives were done by a slightly modified protocol as described below.

In the binding assay on VBP-129, proteins were dialyzed against a buffer (100 mM NaCl, 10 mM Tris-HCl, pH 7.5; here we term it as a buffer A). Vanadyl sulfate (V^{IV}; $VOSO_4 \cdot n\ H_2O$, n = 3-4) was dissolved in DW at 1 mM immediately prior to use. After mixing the proteins with the appropriate amount of 10×concentrated stock of the buffer A, the vanadium solution was added and the mixture was incubated for 5 – 10 min at room temperature. Longer incubation up to 3 h did not gave any significant changes in ESR spectrum. The mixture was placed in a quartz tube (5 × 100 mm, ST-X-5, Agri Co.) and frozen immediately in liquid nitrogen. ESR signals were recorded using the ELEXSYS-II E500 CW-ESR (Bruker BioSpin) with ER 4112V temperature control system at the N-BARD. The sample was inserted into the quartz dewar, which was held in a steam of temperature controlled nitrogen gas. ESR measurements were done at 78 – 80 K with a frequency of 9.4 GHz and a modulation (100 kHz) of 1 mT. Modulation amplitude was 10G, and receiver gain was 60 dB. Conversion time was 15ms. Microwave attenuation was 25 dB, and microwave power was 0.6325W. Number of scan was 3 times. There have been no significant differences among spectra recorded between 78 and 80 K. ESR parameters ($A_{\|}$, $g_{\|}$) were obtained from the spectrum.

In the reduction assay on VBP-129, sodium orthovanadate (99.98% Na_3VO_4, Sigma Aldrich) was dissolved in DW at 10 mM. The yellowish solution was incubated at 60°C until it became colorless. The protein solution was mixed with vanadate solution and the appropriate amount of 10×concentrated stock of the buffer A to give the same buffer composition as the buffer A (100 mM NaCl, 10 mM Tris-HCl, pH 7.5). The mixed solution was incubated at 20°C for 8 h. The solution was then frozen in liquid nitrogen and ESR signals were recorded as described above.

2.6 Determining V^{IV}-binding parameters from ESR intensities

For determining the binding number and dissociation constant for V^{IV} and a protein, relative ESR intensity for a specific resonance was integrated from each ESR spectrum. Assumed that a protein possesses multiple V^{IV}-binding sites (n), a portion of the sites (q) were occupied by the metal ions by equilibrium. Using the total concentrations of vanadium (v) and protein (p), the dissociation constant (K_d) can be calculated with the following equation:

$$Kd = \frac{[VO][site]}{[VOsite]} = \frac{(v-q)(np-q)}{q}$$

At physiological pH and in the absence of coordinating ligands, free V^{IV} is ESR-silent due to the formation of vanadyl hydroxides with various stoichiometries [25]. As shown in Fig. 4A, non-protein-bound V^{IV} ions give little signal at the position of 3/2⊥ peak. Therefore, we chose this peak for intensity analysis. Assuming free vanadium ions were in excess and signals from non-protein-bound V^{IV} ions can be neglected at this pH [25], ESR signal at 3/2⊥ is mostly derived from the occupied sites (*q*). Therefore, ESR intensity (*I*) can be approximated to be proportional to *q*:

$$q = \frac{Kd + v + np - \sqrt{(Kd + v + np)^2 - 4npv}}{2}$$

$$I \equiv cq = c \times \frac{Kd + v + np - \sqrt{(Kd + v + np)^2 - 4npv}}{2}$$

In this equation, *c* is a coefficient to normalize the ESR intensity. By varying *v* and *p*, experimental data were obtained for *I*. Then, the best-fitting parameters, *c*, *n* and K_d, were calculated by repeating Monte Calro algorithm using the Pro Fit software running on a Macintosh OSX (QuantumSoft, Switherland).

3. Results

3.1 Metal-binding ability of VBP-Int41, VBP-N52 and VBP-Int55

In the previous study, a truncated form of VBP-129 that does not bind to V^{IV} was discovered. It has been called VBP-88 for its lack of internal 41 amino acid residues [20]. We thought it should be a starting point to reveal V^{IV}-binding domain(s) in VBP-129. In this study, a recombinant protein with the internal 41-amino-acid sequence between VBP-129 and VBP-88 was first constructed (VBP-Int41; Fig. 1). VBP-Int41 was applied to IMAC chelated with Ca^{II}, Co^{II}, Cu^{II}, Fe^{III}, Mg^{II}, Mn^{II}, V^{IV}, or Zn^{II} ions. Proteins bound with each immobilized metal ion were recovered and analyzed by SDS-PAGE. As a result, VBP-Int41 was found to bind with Co^{II}, Cu^{II}, Fe^{III}, Mn^{II}, and Zn^{II}, but not with V^{IV} ions

(Fig. 2). This result suggested that the internal sequence, VBP-Int41, was insufficient for binding of V^{IV} ions.

Given that VBP-Int41 did not bind to V^{IV}, we hypothesized that neighboring amino acids were necessary for its binding. To test this, we constructed VBP-N52 and VBP-Int55 recombinant proteins by adding neighboring amino acids to VBP-Int41 (Fig. 1). VBP-N52 extends up to the N-terminus of mature VBP-129 by adding 11 amino acid residues. The VBP-Int55 sequence included 14 amino acids that cover the putative α-helical region. Both proteins were applied to IMAC and were found to have an ability to bind V^{IV} as well as to Co^{II}, Cu^{II}, Fe^{III}, Mn^{II}, and Zn^{II} ions (Fig. 2). This data suggested that 52 or 55 amino acid regions are sufficient for V^{IV}-binding.

3.2 Metal-binding abilities of VBP-Int55 and VBP-129 with point mutations

We hypothesized that the 14 amino acids form an important domain for V^{IV}-binding in VBP-Int55 because the additional sequence included lysines and cysteines, which have been shown to be responsible for maintaining the structure and function of another vanadium-binding protein Vanabin2 [21-23]. Thus, we next created two mutants of VBP-Int55 with mutated residues at cysteine-47 and lysine-50, substituting them with serine (VBP-Int55 (C47S)) and alanine (VBP-Int55 (K50A)), respectively. IMAC results indicated that VBP-Int55 (C47S) bound to Co^{II}, Cu^{II}, Fe^{III}, Mn^{II}, and Zn^{II} ions but lost the V^{IV}-binding ability (Fig. 3). VBP-Int55 (C47S) also lost their V^{IV}-binding ability. This suggested that both cysteine-47 and lysine-50 in VBP-Int55 play an important role in binding V^{IV} ions.

To test whether these two amino acid residues were responsible for V^{IV}-binding in the full-length VBP-129, we created the mutants VBP-129(C80S) and VBP-129(K83A). VBP-129(K83A) bound to V^{IV} in addition to Co^{II}, Cu^{II}, Fe^{III}, Mn^{II}, and Zn^{II} ions (Fig. 3). This spectrum of selectivity was similar to the original VBP-129. Thus, the mutation in lysine-83 did not affect the overall ability of VBP-129 to bind V^{IV} ions and its binding differed from VBP-Int55(K50A). On the other hand, VBP-129(C80S) retained its ability to bind to Co^{II}, Cu^{II}, Fe^{III}, Mn^{II}, and Zn^{II}, but V^{IV}-binding was very weak (Fig. 3). This suggested that the mutated cysteine-80 affected the overall ability of VBP-129 to

bind V^{IV} ions.

3.3 ESR measurement of V^{IV}-binding in VBP-129 and its deletion mutants

ESR measurements were performed to determine binding number and dissociation constants between VBP-129 and V^{IV} ions. A constant concentration (14 μM) of VBP-129 was mixed with 0–150 μM V^{IV} in a buffer containing 100mM NaCl and 10 mM Tris-HCl, pH 7.5. Results showed that the complex V^{IV}–VBP-129 invariably exhibited a normal mononuclear-type V^{IV} signal (Fig. 4). At physiological pH and in the absence of coordinating ligands, free V^{IV} is ESR-silent due to the formation of vanadyl hydroxides with various stoichiometries [25], and the ESR signals are from protein-bound V^{IV}. The protein-only sample showed a very weak signal due to crystal imperfections of quartz of the temperature regulating equipment, and the intensity of which was subtracted before calculating the intensity. The curve fitting data indicated that VBP-129 can bind up to 5.6 vanadium per protein with a dissociation constant of 3.8×10^{-6} M (Fig. 5A, Table 2). The ESR parameters of V^{IV}–VBP-129 were $g_{\|} = 1.952$ and $A_{\|} = 168.3\times10^{-4}$ cm^{-1} (Table 3), at the boundary region of the N_2O_2 and $O_2O_2^-$ equatorial donor sets in the $g_{\|}$-$A_{\|}$ diagram [24] . If we assume that lysine(s) contribute as a binding site and $A_{\|}$ is a sum of four equatorial donor sets including amino acid side chains (R-NH_2 = 40.1×10^{-4} cm^{-1}, R-COO^- = 42.7×10^{-4} cm^{-1}) and water molecule (H_2O = 45.7×10^{-4} cm^{-1}) [25, 26], a combination of R-NH_2:R-COO^-:H_2O=2:1:1 (sum = 168.6×10^{-4} cm^{-1}) was closest to the measured $A_{\|}$ value. It is possible that histidine(s) and tyrosine(s) could contribute as binding site(s), but the number of these amino acids in VBP-129 are not enough to make a binding model that could explain a uniform increase of ESR intensity without changing $A_{\|}$. But still, it is possible that histidine can contribute some of the binding sites because the contribution of imidazole nitrogen of a histidine to $A_{\|}$ is similar to that of a lysine [26].

We have also performed the same ESR analysis on the two deletion mutants, VBP-N52 and VBP-Int55 (Fig. 5B and 5C). Here we also describe the ESR data for another vanadium-binding protein Vanabin1 isolated from the same ascidian species (Fig. 5D) [16]. The results were summarized

in Tables 2 and 3. The coordination geometry of V^{IV} in both proteins were similar to original VBP-129. It is also similar to that of Vanabin1 as determined here, and that of Vanabin2 [22].

3.4 Reduction of V^{V} by VBP-129

Recently, our group reported that Vanabin2 can act as a V^{V}-reductase in a thiol-disulfide exchange reaction cascade that included GSH and NADPH [27]. To examine the possibility that such a reduction can occur in blood plasma, we performed ESR analysis to examine V^{V}-reductase activity of VBP-129 as described previously. The reaction cascade in this analysis corresponded to the right half of the cascade (Fig. 4 in ref. 27) starting from reduced GSH through the reduction of V^{V}.

When orthovanadate was incubated with glutathione at 20°C for 8 h, we observed some signals which is different from that of V^{IV} (Fig. 6B, D). We could not attribute the signals to any components. The mixture composition (Fig. 6B) was essentially same as that in our previous work (Fig. 3A spectrum2 in ref. 27) but the signals were very different. Incubation time, buffer composition and measurement temperature were different from each other. Some contaminating materials may affect the spectrum.

When 10 μM of VBP-129 was included in each reaction, the resulting peaks were not significantly different from those without VBP-129 (Fig. 6A, C). The mixture composition was same as that in our previous study (Fig. 3A spectrum 3 in ref. 27) (10 μM Vanabin2 in previous study vs. 10 μM VBP-129 in this work). These results indicated that VBP-129 did not act as a V^{V}-reductase under these experimental conditions.

4. Discussion

Most of the vanadium ions accumulated in ascidians are ultimately localized in the vacuoles of vanadocytes [5]. However, the mechanism by which these ions are taken in before entry into these cells has not been completely determined. Vanadium-binding proteins found in the digestive system,

*As*GST [15, 28], and those in blood plasma, VanabinP and VBP-129 [18, 20], presumably play important roles in the accumulation process. The present study focused on the vanadium-binding protein in blood plasma (VBP-129) and its truncated form (VBP-88), which were suitable starting points to identify V^{IV}-binding domains, based on the affinity for V^{IV} ions in the former, but the lack of binding in the latter [20]. In this study, we constructed several deletion and point mutants of VBP-129, examined the V^{IV}-binding properties of them, and found that VBP-129 binds up to 6 V^{IV} ions in the N_2O_2 coordination geometry. We also found that VBP-129 does not act as V^{V}-reductase.

The 41-amino-acid region found in VBP-129, but not in VBP-88, was named VBP-Int41 (Fig. 1). As shown in Figure 2, VBP-Int41 could not bind V^{IV}, but did bind Co^{II}, Cu^{II}, Fe^{III}, Mn^{II}, and Zn^{II}. In contrast, VBP-Int55 could bind V^{IV} as well as the other five metal ions. VBP-N52 also showed similar properties to VBP-Int55 (Fig. 2). Specifically, VBP-Int41 was incapable of binding to V^{IV} without the flanking amino acid residues.

The ESR results in this study revealed the coordination geometry of V^{IV} in VBP-N52 and VBP-Int55 as well as VBP-129 as the N_2O_2 equatorial donor sets (Table 3). The coordination geometries of V^{IV} in VBP-129, VBP-N52 and VBP-Int55 were very close to that found in the vanadium-binding protein Vanabin2, whose parameters were $g_{\|} = 1.943$ and $A_{\|} = 168.7 \times 10^{-4}$ cm^{-1} [22]. Also, we revealed in this study that those parameters of Vanabin1 were very close to these values. Thus, this type of coordination, a possible combination of ligands of $R\text{-}NH_2$:$R\text{-}COO^-$:H_2O=2:1:1 (calc. sum = 168.6×10^{-4} cm^{-1}), is common to vanadium-binding proteins in ascidians. It should be noted that the additivity of $A_{\|}$ is not unique and further studies should be used to confirm the assignments.

ESR spectrometry has been extensively used to determine the coordination environment around V^{IV} in several vanadium-binding proteins identified from other animals. Table 3 summarizes the axial parameter data on the proteins whose X-band ESR parameters are obtained in a frozen aqueous solution [22, 29-31]. The parameters for VBP-129 are close to those of other vanadium-binding proteins, Vanabin1 and Vanabin2 [22], found in the same species of ascidian. They are also close to A site of human transferrin [29, 32, 33]. Although the coordination geometry for Fe^{III} in this site has been revealed to be Tyr:His:Asp:hydrogencarbonate=2:1:1:1 by X-ray crystalography [34, 35] and the site is common to V^{IV} and Fe^{III} [33], it is still not clear whether same set of amino acid residues bind to

both V^{IV} and Fe^{III} at this site.

In vitro mutagenesis study suggested that lysine-50 in VBP-Int55 plays an important role in binding V^{IV} ions. Because the mutation in lysine-50 diminished V^{IV}-binding and ESR titration revealed that the maximum binding number for V^{IV} is two per molecule of VBP-Int55, the lysine-50 in VBP-Int55 could make a site for binding two V^{IV} ions. Another possibility is that lysine-50 makes a site for a single V^{IV} ion and the mutation also affect the putative secondary site. The latter is more probable because there have been no report for the coordination of two V^{IV} ions per one lysine side chain. The corresponding mutation in VBP-129 (K83A) did not diminish binding to V^{IV}. Based on the ESR results that VBP-129 could bind to six V^{IV} ions, it is possible that lysine-50 contributed only to the binding sites for two of V^{IV} ions and remaining ions bound to site(s) that are only formed in the full-length VBP-129, but not in VBP-88 or VBP-Int55. Another deletion mutant, VBP-N52, was revealed to bind up to three V^{IV} ions in relatively high affinity. It is important to further analyze the role of each amino acid, especially glutamate and aspartate, in the N-terminal stretch in binding activity. A possible binding model is given in Fig. 7. In this model, we assumed that a single molecule of VBP-129 could bind to 6 V^{IV} ions. Cross binding between two or more molecules of VBP-129 could be possible. We have found in our previous study that recombinant VBP-129 could polymerize [20], but the relationship between polymerization and metal-binding is not clear.

Cysteines are involved in the maintenance of structure and V^{V}-reduction in Vanabin2, which contains 18 cysteines. In this study, mutagenesis studies suggested that cysteine-47 in VBP-Int55 (cysteine-80 in VBP-129) plays an important role in binding V^{IV} (Fig. 3) and VBP-129 did not act as a V^{V}-reductase (Fig. 6). According to ESR parameter analysis (Table 3), the role of this cysteine residue is not as a V^{IV}-binding site. Thus, the cysteines may contribute to the maintenance of the three-dimensional structure that is necessary for binding V^{IV} ions. Future studies are recommended to determine the status of disulfide bridges in VBP-129.

VBP-129 can interact with VanabinP, which can bind both V^{IV} and V^{V} ions [18]. VBP-129 and VanabinP form a stable complex, regardless of metal conditions [20]. Although transfer of vanadium ions between VBP-129 and VanabinP has not been determined, these two proteins may act together to deliver V^{IV} ions. V^{V} reduction by VanabinP and subsequent cooperative transport of V^{IV} by a

VanabinP–VBP-129 complex could occur and to be determined in future studies.

Identifying the domain responsible for protein-protein interaction with VanabinP is also needed to further understand the transport mechanism. We were unable to develop a model of the protein structure because no suitable base model was found for VBP-129. We are currently developing solutions to determining the three-dimensional structure experimentally by NMR, which will help us to better understand structure-function relationships.

Approaches such as deletion and point mutagenesis are frequently used to identify protein domains or regions responsible for specific function. *In vitro* point mutagenesis studies are too numerous to be fully elaborated. Studies on the function of N-terminal metal binding sites in P_{1B}-type ATPases, such as Wilson and Menkes proteins in humans, are good examples of the use of deletion mutagenesis [36]. Copper binding sites in amyloid β protein were also extensively studied by a series of deletion mutants [37]. The domains for binding to DNA by nuclear proteins, protein-protein interaction, and secretion have also been studied using this technique [38-40]. These approaches are complementary to determining three-dimensional structure and help establishing structure-function relationships.

In summary, we revealed the V^{IV}-binding domain and the V^{IV}-binding capabilities of VBP-129 as well as the contribution of crucial amino acids for the binding of V^{IV}. We found that VBP-129 binds up to six V^{IV} ions and the coordination geometry was N_2O_2 donor sets, possibly composed of a combination of ligands of $R\text{-}NH_2$:$R\text{-}COO^-$:H_2O=2:1:1 ($A_{\parallel}$ calculated = 168.6×10^{-4} cm^{-1}). Because we did not obtain any evidence of V^V reduction by VBP-129, it was suggested that VBP-129 acts solely as a V^{IV}-carrier in blood plasma that delivers V^{IV} ions to target proteins in some tissue(s) or cell(s).

Abbreviations

BSA	bovine serum albumin
CBB	coomassie brilliant blue
CW-ESR	constant-wave electro spin resonance
DEAE	diethylaminoethyl
DW	deionized pure water

EDTA	ethylenediaminetetraacetic acid
ENDOR	electron nuclear double resonance)
ESR	electron spin resonance
ESEEM	electron spin-echo envelope modulation
IMAC	immobilized metal ion affinity chromatography
IPTG	isopropyl-β-d-thiogalactopyranoside
LB-Amp	Luria-Bertani broth supplemented with ampicillin
MBP	maltose binding protein
NMR	nuclear magnetic resonance
PCR	polymerase chain reaction
SDS-PAGE	sodium dodecyl sulfate polyacrylamide gel electrophoresis
Tris	tris(hydroxymethyl)aminomethane

Acknowledgments

We thank Prof. Manabu Abe, Department of Chemistry, Graduate School of Science, Hiroshima University, for his help with ESR measurements, which were accomplished using the ELEXSYS-II E500 CW-ESR instrument at the Natural Science Center for Basic Research and Development (N-BARD), Hiroshima University. We also thank Dr. Koichi Fukui for his help with ESR measurements and curve fitting analyses. This work was supported in part by Grants-in-Aid from the Ministry of Education, Culture, Sports, Science and Technology, Japan (nos. 20570070 and 21570077).

References

[1] M. Henze, Untersuchungen über das Blut der Ascidien. I. Mitteilung, Hoppe-Seyler's Z. Physiol. Chem. 72 (1911) 494-501.

[2] H. Michibata, T. Terada, N. Anada, K. Yamakawa, T. Numakunai, Biol. Bull. 171 (1986) 672-681.

[3] J. Hirata, H. Michibata, J. Exp. Zool. 257 (1991) 160-165.

[4] H. Michibata, Y. Iwata, J. Hirata, J. Exp. Zool. 257 (1991) 306-313.

[5] T. Ueki, K. Takemoto, B. Fayard, M. Salome, A. Yamamoto, H. Kihara, J. Susini, S. Scippa, T. Uyama, H. Michibata, , Zool. Sci. 19 (2002) 27-35.

[6] T. Uyama, Y. Moriyama, M. Futai, H. Michibata, J. Exp. Zool. 270 (1994) 148-154.

[7] T. Ueki, T. Uyama, K. Kanamori, H. Michibata, Zool. Sci. 15 (1998) 823-829.

[8] T. Ueki, T. Uyama, K. Kanamori, H. Michibata, Mar. Biotechnol. 3 (2001) 316-321.

[9] T. Ueki, N. Yamaguchi, H. Michibata, Comp. Biochem. Physiol. B Biochem. Mol. Biol. 136 (2003) 91-98.

[10] T. Ueki, N. Furuno, Q. Xu, Y. Nitta, K. Kanamori, H. Michibata, Biochim. Biophys. Acta 1790 (2009) 1295-1300.

[11] T. Uyama, T. Kinoshita, H. Takahashi, N. Satoh, K. Kanamori, H. Michibata, J. Biochem. 124 (1998) 377-382.

[12] T. Uyama, T. Ueki, Y. Suhama, K. Kanamori, H. Michibata, Zool. Sci. 15 (1998) 815-821.

[13] T. Uyama, K. Yamamoto, K. Kanamori, H. Michibata, Zool. Sci. 15 (1998) 441-446.

[14] T. Ueki, T. Uyama, K. Yamamoto, K. Kanamori, H. Michibata, Biochim. Biophys. Acta 1494 (2000) 83-90.

[15] M. Yoshinaga, T. Ueki, H. Michibata, Biochim. Biophys. Acta 1770 (2007) 1413-1418.

[16] T. Ueki, T. Adachi, S. Kawano, M. Aoshima, N. Yamaguchi, K. Kanamori, H. Michibata, Biochim. Biophys. Acta 1626 (2003) 43-50.

[17] N. Yamaguchi, K. Kamino, T. Ueki, H. Michibata, Mar. Biotechnol. (NY) 6 (2004) 165-174.

[18] M. Yoshihara, T. Ueki, T. Watanabe, N. Yamaguchi, K. Kamino, H. Michibata, Biochim. Biophys. Acta 1730 (2005) 206-214.

[19] T. Ueki, N. Furuno, H. Michibata, Biochim Biophys Acta 1810 (2011) 457-464.

[20] M. Yoshihara, T. Ueki, N. Yamaguchi, K. Kamino, H. Michibata, Biochim. Biophys. Acta 1780 (2008) 256-263.

[21] T. Ueki, N. Kawakami, M. Toshishige, K. Matsuo, K. Gekko, H. Michibata, Biochim. Biophys. Acta 1790 (2009) 1327-1333.

[22] K. Fukui, T. Ueki, H. Ohya, H. Michibata, J. Am. Chem. Soc. 125 (2003) 6352-6353.

[23] T. Hamada, M. Asanuma, T. Ueki, F. Hayashi, N. Kobayashi, S. Yokoyama, H. Michibata, H. Hirota, J. Am. Chem. Soc. 127 (2005) 4216-4222.

[24] H. Sakurai, J. Hirata, H. Michibata, Biochem. Biophys. Res. Commun. 149 (1987) 411-416.

[25] N.D. Chasteen, in: L.J. Berliner, J. Reuben (Eds.) Biological magnetic resonance, vol. 3, Plenum Press, New York, 1981, pp. 53-119.

[26] T. Smith, R. Lobrutto, V. Pecoraro, Coord. Chem. Rev., 228 (2002) 1-18.

[27] N. Kawakami, T. Ueki, Y. Amata, K. Kanamori, K. Matsuo, K. Gekko, H. Michibata, Biochim.

Biophys. Acta 1794 (2009) 674-679.

[28] M. Yoshinaga, T. Ueki, N. Yamaguchi, K. Kamino, H. Michibata, Biochim. Biophys. Acta 1760 (2006) 495-503.

[29] D. Sanna, E. Garribba, G. Micera, J. Inorg. Biochem. 103 (2009) 648-655.

[30] N.D. Chasteen, E.C. Theil, J. Biol. Chem. 257 (1982) 7672-7677.

[31] D. Sanna, G. Micera, E. Garribba, Inorg. Chem. 50 (2011) 3717-3728.

[32] J.C. Cannon, N.D. Chasteen, Biochemistry 14 (1975) 4573-4577.

[33] D.C. Harris, Biochemistry 16 (1977) 560-564.

[34] D.R. Hall, J.M. Hadden, G.A. Leonard, S. Bailey, M. Neu, M. Winn, P.F. Lindley, Acta Crystallogr. D Biol. Crystallogr. 58 (2002) 70-80.

[35] P. Guha Thakurta, D. Choudhury, R. Dasgupta, J.K. Dattagupta, Acta Crystallogr. D Biol. Crystallogr. 59 (2003) 1773-1781.

[36] D. Huster, S. Lutsenko, J. Biol. Chem. 278 (2003) 32212-32218.

[37] J.W. Karr, H. Akintoye, L.J. Kaupp, V.A. Szalai, Biochemistry 44 (2005) 5478-5487.

[38] K. Hingorani, A. Szebeni, M.O. Olson, J. Biol. Chem. 275 (2000) 24451-24457.

[39] T.L. Johnson, M.E. Scott, M. Sandkvist, J. Bacteriol. 189 (2007) 9082-9089.

[40] D. Gell, S.P. Jackson, Nucleic Acids Res. 27 (1999) 3494-3502.

[41] H. Michibata, T. Ueki, Biomolec. Concep. 1 (2010) 97-107.

[42] H. Michibata, N. Yamaguchi, T. Uyama, T. Ueki, Coord. Chem. Rev. 237 (2003) 41-51.

[43] H. Michibata, M. Yoshinaga, M. Yoshihara, N. Kawakami, N. Yamaguchi, T. Ueki, in: K. Kustin, J. Costa-Pessoa, D.C. Crans (Eds.) Vanadium the Versatile metal, Oxford University Press, Oxford, 2007, pp. 264-280.

Table 1. List of primer sets and templates used for construction of VBP-129 mutants.

Protein name	Primers [a)]	Templates [b)]
VBP-Int41	5'-GGAATTCCTGTCCGATTGCATCC-3'	pMAL-p2X:VBP-129
	5'-GGAATTCCTGTCCGATTGCATCC-3'	
VBP-N52	5'-GGATCCCTGGGAAGCGATGCT-3'	pMAL-p2X:VBP-129
	5'-CGTCGACTCATTTTAGGCGAAGT-3'	
VBP-Int55	5'-GGAATTCCTGTCCGATTGCATCC-3'	pMAL-p2X:VBP-129
	5'- CGTCGACTCAAATTCTT TCGGTGT-3'	
VBP-Int55(C47S) or	5'-AATGCGCCAAAGCCTTAACAAAT-3'	pMAL-c2X:VBP-Int55 or
VBP-129(C80S)	5'-ATTTGTTAAGGCTTTGGCGCATT-3'	pMAL-p2X:VBP-129
VBP-Int55(K50A) or	5'-ATGCCTTAACGCATACACCGAAAG-3'	pMAL-c2X:VBP-Int55 or
VBP-129(K83A)	5'-CTTTCGGTGTATGCGTTAAGGCATT-3'	pMAL-p2X:VBP-129

[a)] Primers for deletion mutants include artificial restriction sites (underlined). Primers for point mutants include mutagenizing codon in their central region (double-underlined).

[b)] Template plasmid DNAs are derived from the previous study [20].

Table 2. ESR titration for the V^{IV}-binding to vanadium-binding proteins VBP-129, its deletion mutants and Vanabins.

	N_{max}	K_d (M)	reference
VBP-129	5.6	3.8×10^{-6}	this study
VBP-N52	2.7	0.99×10^{-6}	this study
VBP-Int55	2.0	8.2×10^{-6}	this study
Vanabin1	15	$< 0.1 \times 10^{-6}$	this study
Vanabin2	24	$< 0.1 \times 10^{-6}$	[22]

Table 3. ESR parameters for the V^{IV} complexes formed by proteins.

	$g_{\|}$	$A_{\|}$ ($\times 10^{-4}$ cm^{-1})	reference
VBP-129	1.952	168.3	this study
VBP-N52	1.947	167.4	this study
VBP-Int55	1.954	168.9	this study
Vanabin1	1.946	169.2	this study
Vanabin2	1.943	168.7	[22]
hTf, A site	1.937	168.3	[29]
hTf, B1 site	1.941	170.5	[29]
hTf, B2 site	1.935	171.8	[29]
HSA, weak site	1.946	171.2	[29]
HSA, strong site	1.947	164.6	[29]
HSF	1.940	173.0	[30]
IgG, site 1	1.960	158.8	[31]
IgG, site 2	1.951	163.6	[31]
IgG, site 3	1.947	167.4	[31]

hTf: human transferrin, HSA, human serum albumin, HSF: horse spleen ferritin, IgG: Immunoglobulin G.

Figure legends

Fig. 1. Amino acid sequences of VBP-129 and its deletion mutants. Lower-case characters indicate signal sequences. Mutated sites are boxed. Asterisks indicate putative helical domains. Lysines (K) are shown in blue, while aspartic acid and (D) and glutamic acids (E) are shown in red.

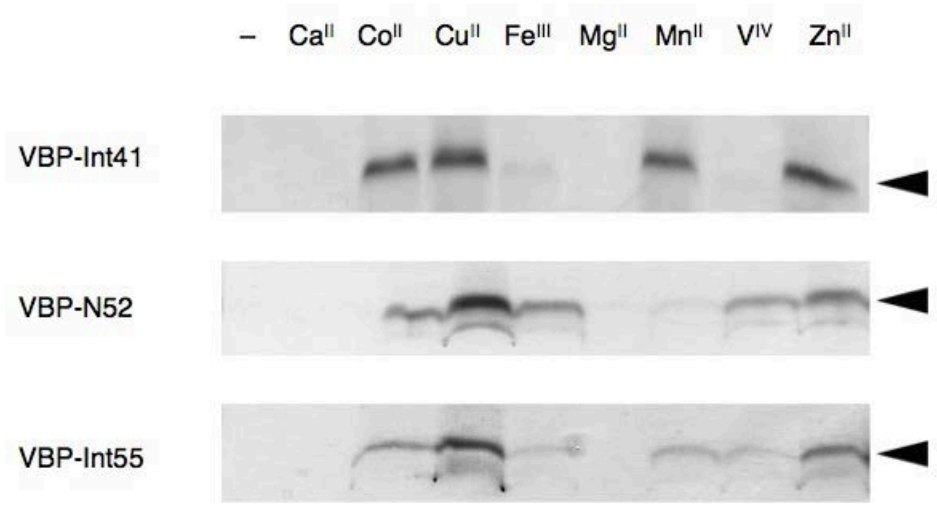

Fig. 2. IMAC analysis of metal binding by deletion mutants of VBP-129. The metal-binding experiment was performed using 100 mM NaCl and 20 mM Na_3PO_4 at pH 7.2. Recombinant proteins were applied to IMAC charged with metal ions indicated at the top or without any metal ions (–), respectively, and incubated for 30 min at 4°C. After removal of non-bound proteins, the metal-bound fraction was eluted with EDTA-containing buffer, as described in the Materials and Methods. Protein fractions were analyzed by SDS-PAGE and CBB staining. Arrowheads indicate the protein bands.

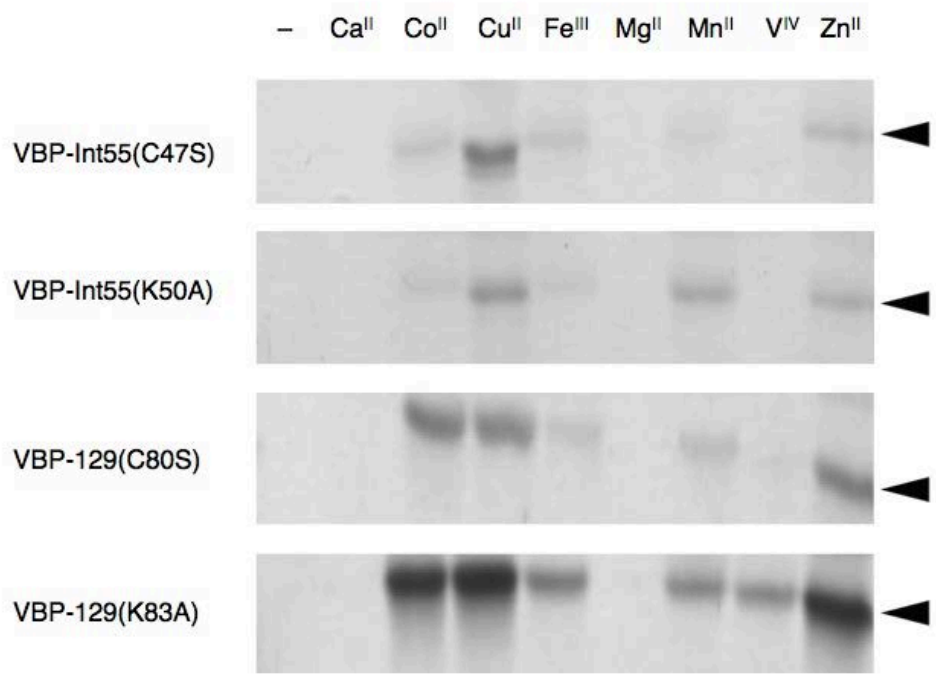

Fig. 3. IMAC analysis of metal binding by point mutants of VBP-Int55 and VBP-129. The metal-binding experiment was performed using 100 mM NaCl and 20 mM Na_3PO_4 at pH 7.2. Recombinant proteins were applied to IMAC charged with metal ions indicated at the top or without any metal ions (–), respectively, and were examined as in **Fig. 2**. Arrowheads indicate the protein bands.

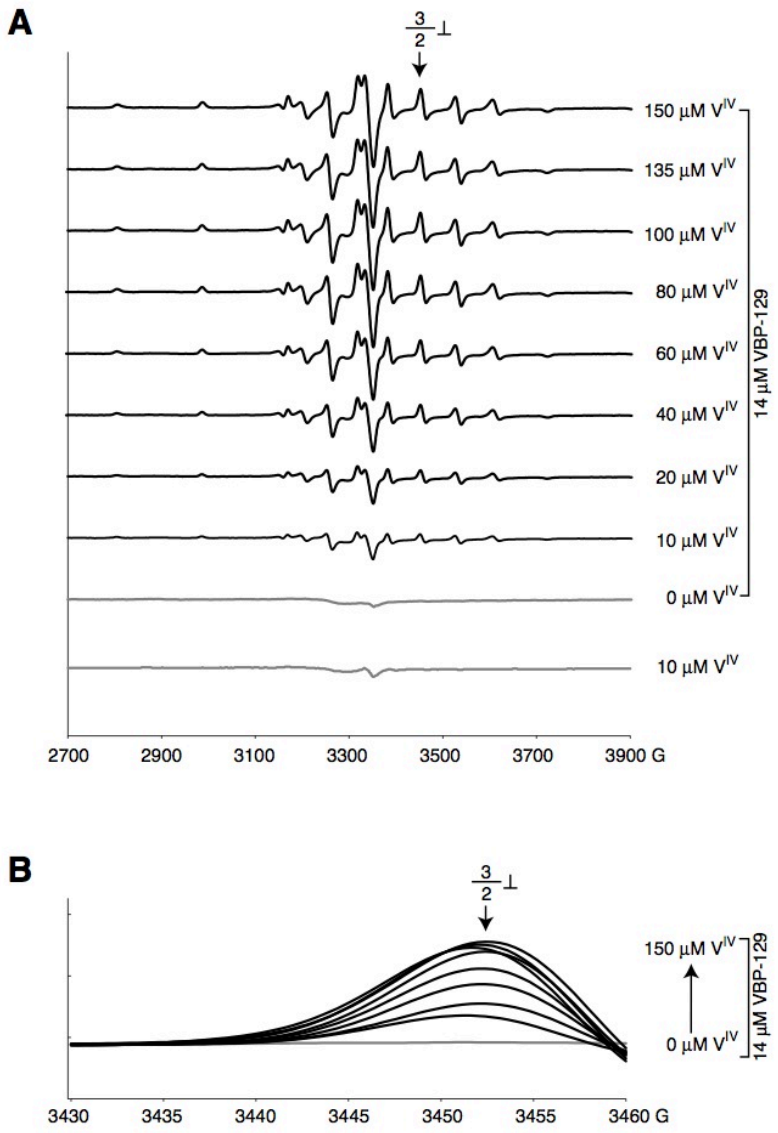

Fig. 4. Representative CW ESR spectra of samples containing various ratios of V^{IV} and VBP-129. **(A)** Spectra recorded from 2700 G to 3900 G. The arrow indicates the ^{51}V hyperfine line ($3/2_{\perp}$). V^{IV}-only sample (10 μM V^{IV} without protein) and protein-only sample (0 μM V^{IV}, 14 μM VBP-129) are included as references. **(B)** Magnified overwrapped spectra for the ^{51}V hyperfine line ($3/2_{\perp}$) in **(A)**. The intensity of protein-only sample (0 μM V^{IV}) has been subtracted from each spectra. Conditions: *T* = 79 K; microwave frequency, 9.4 GHz; microwave power, 1 mW; modulation (100 kHz), 1 mT; Resolutions = 0.4 G per point. Final concentrations: [V^{IV}] =0-150 μM , [VBP-129] = 14 μM, [Tris] = 10 mM, and [NaCl] = 100 mM, pH 7.5, in a total volume of 100 μL.

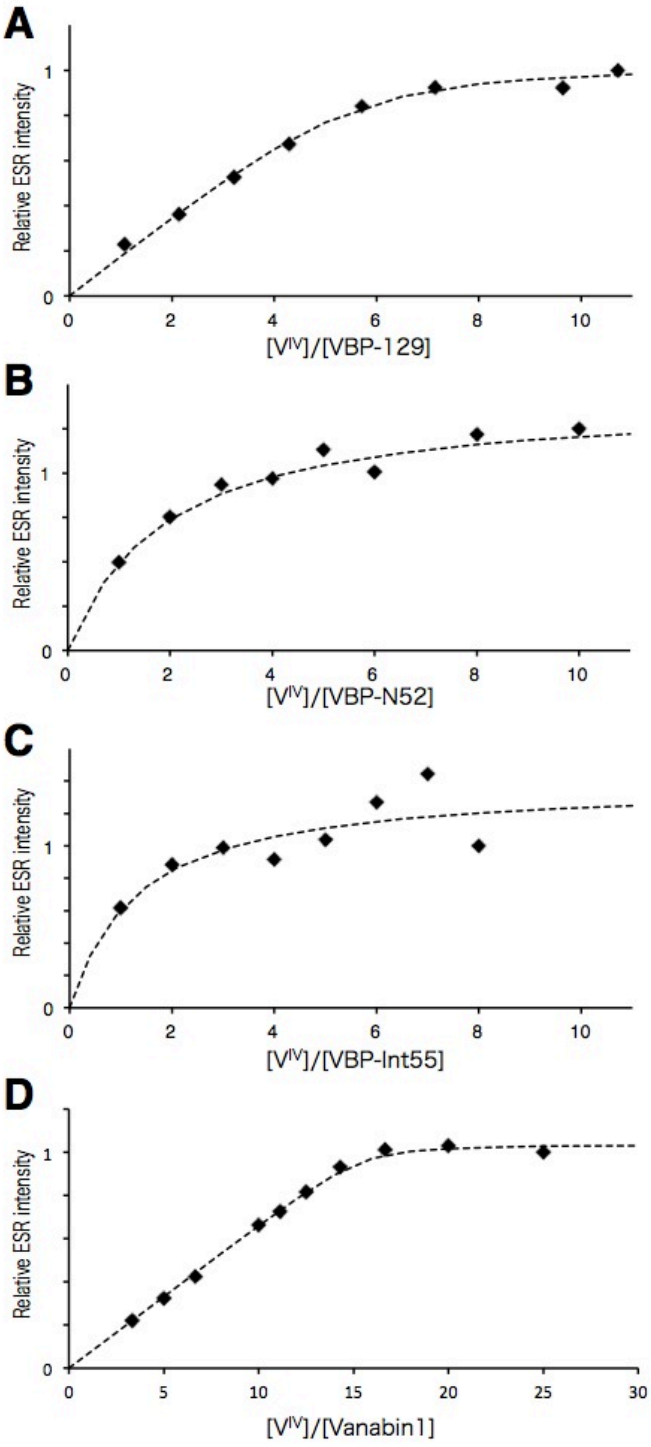

Fig. 5. ESR spectrometric titration of V^{IV} ion bound to **(A)** VBP-129, **(B)** VBP-N52, **(C)** VBP-Int55 and **(D)** Vanbabin1. ESR intensities of the $M_I = 3/2_{\perp}$ lines for various V^{IV} ions per protein ratios are plotted by black diamonds. Dotted lines indicates the best curve fittings whose parameters were summarized in Table 2.

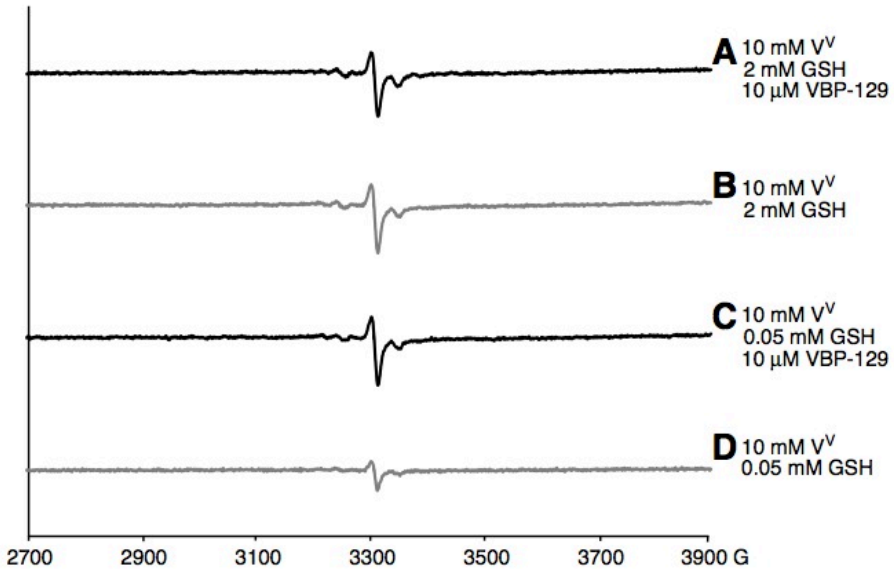

Fig. 6. ESR spectrometric analysis of V^V-reduction by VBP-129. Each component was mixed and incubated at 20°C for 8 h before ESR measurement at 80K. Spectrums: (A), 10 mM V^V + 2 mM GSH + 10 μM VBP-129; (B), 10 mM V^V + 2 mM GSH; (C), 10 mM V^V + 0.05 mM GSH + 10 μM VBP-129; (D), 10 mM V^V + 0.05 mM GSH. Buffer composition was [Tris] = 10 mM, and [NaCl] = 100 mM, pH 7.5. Conditions: T = 79 K; microwave frequency, 9.4 GHz; microwave power, 1 mW; modulation (100 kHz), 1 mT; Resolutions = 0.4 G per point.

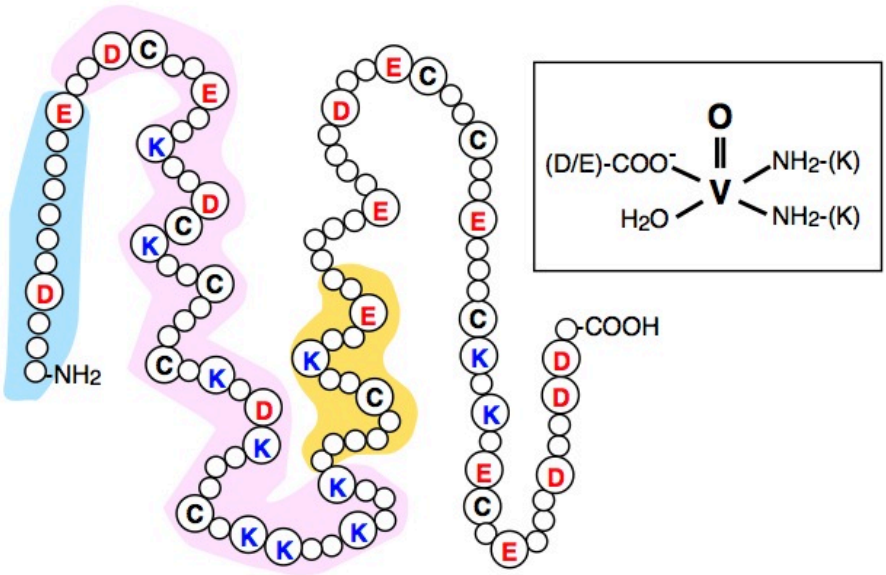

Fig. 7. A possible model of the binding of VBP-129 to V^{IV}. VBP-Int41 (pink) contains 8 lysines (K) and 4 aspartic acid/glutamic acid (D/E), but cannot bind V^{IV} (V). By adding neighboring amino acid residues, VBP-N52 (blue+pink) and VBP-Int55 (pink+yellow) can bind three or two V^{IV} in N_2O_2 geometry, respectively, possibly composed of a combination of ligands of K:(D/E):H_2O=2:1:1. The full-length VBP-129 can additionally bind another V^{IV} by using additional sets of K or D/E in the C-terminal stretch.